

# Calculations of crystal-melt interfacial free energies by nonequilibrium work measurements

Yan Mu and Xueyu Song<sup>a)</sup>

*Department of Chemistry, Iowa State University, Ames, Iowa 50011*

(Received 26 September 2005; accepted 29 November 2005; published online 20 January 2006)

We developed a multistep thermodynamic perturbation method to compute the interfacial free energies by nonequilibrium work measurements with cleaving potential procedure. Using this method, we calculated the interfacial free energies of different crystal orientations for the Lennard-Jones system. Our results are in good agreement with the results by thermodynamic integration method. Compared with thermodynamic integration method, the multistep thermodynamic perturbation method is more efficient. For each stage of the cleaving process, only a few thermodynamic perturbation steps are needed, and there is no requirement on the reversibility of the path. © 2006 American Institute of Physics. [DOI: [10.1063/1.2159474](https://doi.org/10.1063/1.2159474)]

## I. INTRODUCTION

In recent years, there has been a persistent interest focused on the calculations of crystal-melt interfacial free energies due to the fact that the crystal-melt interfacial free energy  $\gamma$  is of significant importance in the crystal growth. Both its magnitude and anisotropy are primary controlling parameters governing the kinetics and morphology of crystal growth. As a consequence, it is highly desirable to accurately measure or predict this quantity. However, it is difficult to measure the crystal-melt interfacial free energy  $\gamma$  accurately and efficiently.<sup>1,2</sup>

Experimentally, the crystal-melt interfacial free energy  $\gamma$  can be estimated through measurements of crystal nucleation rates<sup>3–6</sup> or direct measurements via Wulff construction.<sup>7,8</sup> However, the method of measuring crystal nucleation rates cannot be used to determine the anisotropy of the interfacial free energies and the values obtained are not very accurate due to the approximations inherent in the classical nucleation theory. It is also difficult to directly measure the crystal-melt interfacial free energy  $\gamma$  and so far only a few materials have been studied. Thus efficient and accurate theoretical/computational methods will be very useful alternatives to provide reliable information on the crystal-melt interfaces and their interfacial free energies.

Theoretically, the primary approach to calculate the crystal-melt interfacial free energy has been the density-functional theory (DFT).<sup>9–13</sup> However, the value of the interfacial free energy  $\gamma$  obtained depends very much on the approximations used and the density profile parametrizations employed in the DFT studies. Although reliable overall interfacial free energy can be obtained from fundamental measure functional,<sup>14</sup> it is still very difficult to resolve the anisotropy of the interfacial free energies.

The interfacial free energy  $\gamma$  may also be determined from computer simulations. In recent years, two main simulation methods are developed: capillary-wave method<sup>2,15–24</sup>

and cleaving potential technique.<sup>25–27</sup> The capillary-wave method is based on the fact that if the crystal-melt interface of interest is rough, the magnitude of the height fluctuations of the interface between crystal and its melt depends on the stiffness of the interface which is related to the interfacial free energy. Through monitoring the fluctuations in the position of the interfaces, the interfacial stiffnesses can be extracted directly, and subsequently the interfacial free energies can be obtained by solving the equations relating the interfacial stiffnesses and the interfacial free energies. Furthermore, the interfacial stiffness is more anisotropic than the interfacial free energy; thus, the capillary-wave method is more accurate in determining the anisotropy of the interfacial free energies. However, it is difficult for the capillary-wave method to provide very accurate values of the interfacial free energy due to the uncertainties of converting the discrete particle description of the interface from simulations to the continuum description of the capillary-wave method.<sup>24</sup>

In the cleaving potential approach, the crystal-melt interfacial free energy per unit area is defined as the reversible work needed to form a unit area of interface between a crystal and its melt. Broughton and Gilmer<sup>25</sup> used the cleaving potential technique to calculate the reversible work directly in the Lennard-Jones system, but in this early work the computed values of  $\gamma$  were insufficiently accurate to determine the anisotropy of the interfacial free energies. Recently, Davidchack and Laird<sup>26,27</sup> improved the cleaving procedure through the use of a “cleaving wall” consisting of ideal crystal layers. With this modified cleaving technique, they have calculated the interfacial free energies for the hard-sphere and the Lennard-Jones systems using the thermodynamic integration with molecular-dynamics (MD) simulations, and provided sufficient accuracy to resolve the anisotropy of the interfacial free energies. However, it is very time consuming to calculate the interfacial free energies by thermodynamic integration method due to the strict requirement on the reversibility of the integration path to avoid hysteresis.

In this paper, we developed a multistep thermodynamic perturbation method to compute the interfacial free energies

<sup>a)</sup>Electronic mail: [xsong@iastate.edu](mailto:xsong@iastate.edu)

by nonequilibrium work measurements with cleaving potential procedure. Using this method, we calculated the interfacial free energies of different crystal orientations for the Lennard-Jones system. Our results are in good agreement with the results by thermodynamic integration method,<sup>27</sup> and our method seems to be more efficient than thermodynamic integration method as the method does not rely on a reversible path.

The paper is organized in the following way. In Sec. II the basic strategy of the cleaving potential method combining with multistep thermodynamic perturbation method is presented. To reduce the statistical error the Bennett method<sup>28,29</sup> is adopted for the analysis. In Sec. III details of our simulations and analysis are given. Section IV concludes with some remarks on possible applications and extensions of our method.

## II. THE CLEAVING POTENTIAL METHOD WITH NONEQUILIBRIUM WORK MEASUREMENTS

From the second law of thermodynamics, the average work that is needed to change a system from an initial to a final equilibrium state is larger than the Helmholtz free-energy difference between the two equilibrium states:

$$\overline{W} \geq \Delta F. \quad (1)$$

This is an inequality, in general. The equality holds only when the work is performed on the system along a reversible path. This is the basic strategy of the traditional cleaving potential method to compute interfacial free energies between a crystal and its melt.<sup>25-27</sup> However, it is very time consuming to calculate the reversible work by changing the system parameters in an infinitely slow manner, and moreover, it is difficult to design a reversible path to calculate the free-energy difference in most cases.

A few years ago, Jarzynski<sup>30</sup> derived an equality which shows that the equilibrium free-energy difference can be expressed as an exponential average of the work performed on the system:

$$\exp(-\beta\Delta F) = \langle \exp(-\beta W_{i \rightarrow f}) \rangle_i, \quad (2)$$

where  $\beta = 1/kT$  is the reciprocal temperature in energy units and  $\Delta F = F_f - F_i$  is the free-energy difference between the initial and final equilibrium system states.  $W_{i \rightarrow f}$  is the work involved in a process taking the system from the initial to the final state. The angular brackets indicate that the quantity is an ensemble average performed on the initial equilibrium system state  $i$ . This result is independent of both the path from the initial to the final system state and the rate of system parameters changing along the path.

The most remarkable feature of the Jarzynski theorem is that the equilibrium quantity  $\Delta F$  can be extracted from an ensemble of nonequilibrium work measurements, which introduces new ways of calculating equilibrium free-energy difference. This feature has been investigated and exploited in some recent works.<sup>31-36</sup> Since the Jarzynski equality bridges the traditional thermodynamic perturbation method and the thermodynamic integration method as two limiting cases, for various situations, the optimal switching strategy may lie somewhere in between. For the interfacial-free-

energy calculation, we found that a multiple-step thermodynamic perturbation strategy may be the best choice. In this paper, we have applied this strategy to calculate the interfacial free energy combining with the cleaving potential procedure.

### A. The cleaving potential technique

The crystal-liquid interfaces can be created by the following cleaving potential procedure, which is composed of four stages:<sup>27</sup>

- (1) stage 1: split the crystal bulk phase with cleaving walls while maintaining the periodic boundary conditions;
- (2) stage 2: split the liquid phase in a similar way;
- (3) stage 3: juxtapose the cleaved crystal and liquid systems by rearranging the boundary conditions while maintaining the cleaving walls; and
- (4) stage 4: remove the cleaving wall from the combined system.

The cleaving plane is where the crystal and liquid systems are splitted into two parts. The location of the cleaving plane in the crystal must be chosen in the center between two crystal layers, while it is arbitrary in the liquid system. The cleaving walls have repulsive interactions only with the system particles on the opposite side of the cleaving plane. As the cleaving walls move closer to the cleaving plane, the particles are prevented from crossing the cleaving plane and then the system are splitted along the cleaving plane. In order to form an appropriate interfacial layer structure similar to that at the real crystal-liquid interfacial region for the liquid system, the cleaving walls are made of the crystal layers with proper orientation and the cleaving potential is chosen to be similar to the system potential. If the four stages are performed in a very slow manner, the interfacial free energy is the reversible work required in the whole process divided by the area of the created interface. Traditionally the total reversible work was computed by thermodynamic integration method.

Instead of calculating the reversible work with thermodynamic integration method, we can obtain the free-energy difference by computing the nonequilibrium work required to switch the system states by changing the system parameters infinitely fast as Eq. (2) indicates. In practice, if there is a large free-energy gap between the initial and final states, intermediate equilibrium states should be inserted to increase sampling efficiency. The total free-energy difference can be obtained by summing all the free-energy differences between these intermediate states. It can be shown that an intermediate equilibrium state will give the lowest nonequilibrium work and hence yield the most efficient sampling trajectories. In the cleaving process, the equilibrium system states can be defined by a set of discrete system parameters for each stage. In stages 1, 2, and 4, the system parameters correspond to the distance  $x$  between the cleaving wall and cleaving plane, while in step 3, the system parameter corresponds to the coupling parameter  $\lambda$  which describes the degree of the crystal-melt interface formation. Thus, we can

develop a multiple-step thermodynamic perturbation method to calculate the interfacial free energies with the cleaving procedure.

However, straightforward employment of thermodynamic perturbation method tends to give large statistical errors in the results, especially for the cases where the free-energy difference between two equilibrium states is relatively large. In order to minimize the statistical errors of the results, we use the Bennett acceptance ratio method to circumvent such difficulties.

### B. Bennett acceptance ratio method

The Bennett method<sup>28,29</sup> combines the information in both forward and reverse paths to minimize the variance in the calculation of the free-energy difference between two equilibrium states. Assuming that the numbers of work measurements of both forward and reverse paths are the same  $n_F = n_R = n$ , the free-energy difference can be obtained by solving the following self-consistent equation:

$$\sum_F^n \left( \frac{1}{1 + \exp[\beta(W - \Delta F)]} \right) - \sum_R^n \left( \frac{1}{1 + \exp[-\beta(W - \Delta F)]} \right) = 0, \quad (3)$$

where the subscripts  $F$  and  $R$  represent the forward and reverse paths, respectively. The estimated statistical error in  $\Delta F$  is determined by the variance:

$$U_{LJ}(r) = \begin{cases} 4\epsilon \left[ \left( \frac{\sigma}{r} \right)^{12} - \left( \frac{\sigma}{r} \right)^6 \right] + C_1, & r \leq 2.3\sigma, \\ C_2 \left( \frac{\sigma}{r} \right)^{12} + C_3 \left( \frac{\sigma}{r} \right)^6 + C_4 \left( \frac{\sigma}{r} \right)^2 + C_5, & 2.3\sigma < r < 2.5\sigma, \\ 0, & r \geq 2.5\sigma, \end{cases} \quad (5)$$

where  $C_1 = 0.016132\epsilon$ ,  $C_2 = 3136.6\epsilon$ ,  $C_3 = -68.069\epsilon$ ,  $C_4 = -0.083312\epsilon$ , and  $C_5 = 0.74689\epsilon$ . The cleaving potential  $\phi_c(r)$  is

$$\phi_c(r) = \begin{cases} 4\epsilon \left[ \left( \frac{\sigma}{r} \right)^{12} - \left( \frac{\sigma}{r} \right)^6 \right] + \epsilon, & r < r_w = 2^{1/6}\sigma, \\ 0, & r \geq r_w. \end{cases} \quad (6)$$

In our simulations, the initial position of the cleaving wall  $x_i$  is  $1.1\sigma$ , which is large enough to ensure that the cleaving walls do not interact with the system, and the final positions  $x_f$  are  $0.60\sigma$ ,  $0.50\sigma$ , and  $0.65\sigma$  for (100), (110), and (111) crystal orientations, respectively. In addition, we define the work measurement from the low free-energy state to the high

TABLE I. The system geometries and number of particles of fcc crystal bulk phases for different crystal orientations in simulations. The geometries are shown with all lengths in units of  $a = (4/\rho_c)^{1/3}$ , which is the size of the fcc unit cell.

Interface	Geometry	Number of particles
(100)	$20a \times 9a \times 9a$	6480
(110)	$12\sqrt{2}a \times 6\sqrt{2}a \times 9a$	5184
(111)	$12\sqrt{3}a \times 5.5\sqrt{2}a \times 3\sqrt{6}a$	4752

$$\sigma_{\Delta F}^2 = \frac{1}{\beta^2} \left[ \frac{1}{n} \left\langle \frac{1}{1 + \exp[\pm\beta(W - \Delta F)]} \right\rangle_{F(R)}^{-1} - \frac{2}{n} \right], \quad (4)$$

where “ $\pm$ ” in the above equation correspond to the forward and reverse paths, respectively. It can be shown that the Bennett method effectively reduce the statistic error and significantly improves the reliability of the results.<sup>29</sup>

### III. SIMULATION RESULTS AND DISCUSSIONS

In this paper, we calculated the fcc crystal-liquid interfacial free energies of the Lennard-Jones system near the triple-point temperature using Monte Carlo (MC) simulations with  $NVT$  ensemble. First of all, the pure fcc crystal and liquid are prepared separately near the triple-point temperature of  $T = 0.617k_B\epsilon^{-1}$ . At this point the coexistence densities of crystal and liquid are  $0.945\sigma^{-3}$  and  $0.828\sigma^{-3}$ , respectively. Details of system geometries of fcc crystal bulk phases for different crystal orientations are given in Table I. The corresponding liquid phase has the same number of particles. In order to have a direct comparison with the results of Davidchack and Laird,<sup>27</sup> we have used the same modification of the Lennard-Jones potential and the cleaving potential. The modified Lennard-Jones potential  $U_{LJ}(r)$  is

free-energy state as forward direction and the work measurement from high free-energy state to the low free-energy state as reverse direction.

A series of thermodynamic perturbation steps are used to calculate the free-energy difference for each stage. The non-equilibrium works in both forward and reverse paths are computed for each thermodynamic perturbation step, and then they are combined together through Eq. (3) to calculate the free-energy difference in this perturbation step. Figure 1 shows the landscapes of the free-energy differences in stage 2 of cleaving liquid and stage 3 of forming interface for the (100) crystal orientation. In Fig. 1(a), the abscissa  $x$  is the distance between the cleaving wall and cleaving plane,

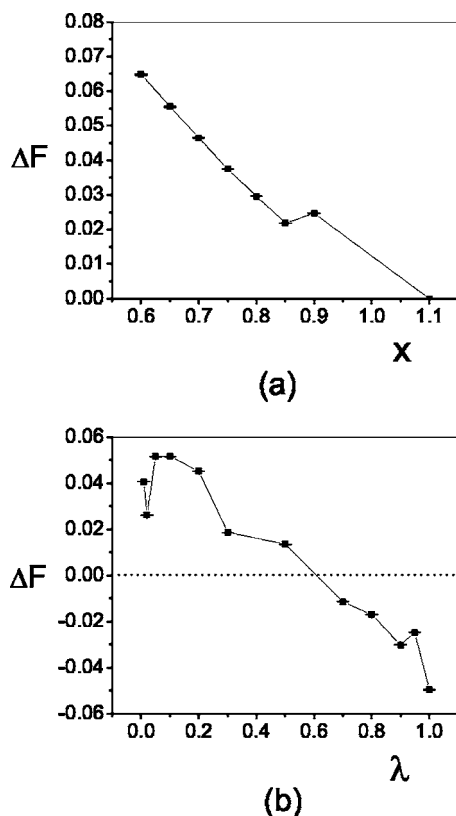


FIG. 1. (a) The landscape of the free-energy difference in stage 2 for the (100) crystal orientation.  $x$  is the distance between the cleaving wall and cleaving plane, which defines the system state. (b) The landscape of the free-energy difference in stage 3 for the (100) crystal orientation.  $\lambda$  is the coupling parameter, which defines the degree of interface formation.

which defines various system states; in Fig. 1(b), the abscissa  $\lambda$  is the coupling parameter of defining the degree of interface formation ( $\lambda=0$  means that the liquid and the crystal phases are not interacting and  $\lambda=1$  means that the two phase are fully interacting). Each point represents the free-energy difference between two neighboring states. The summation of these free-energy differences gives the total free-energy difference in that stage.

The convergence of the free-energy difference in each stage can be tested by varying the number of thermodynamic perturbation steps in that stage. In fact, the number of thermodynamic perturbation steps needed depends on not only free-energy difference between initial and final states but also on system potential. From our calculations for the Lennard-Jones system, we found that when the free-energy difference between two system states is larger than  $0.10k_B T/\sigma^2$ , the Bennett variance becomes very large. In this case, an intermediate state should be inserted to improve the accuracy of the result. In general, different systems may have different criteria. Depending on a particular criterion, we can flexibly design a scheme of calculating the free-energy difference to make the calculations more efficient and accurate for various systems. Figure 2 shows the dependence of the free-energy difference on the number of thermodynamic perturbation steps used in the four stages for the (100) crystal orientation. It can be seen clearly that for stage 1 of cleaving solid, one thermodynamic perturbation step is enough to get

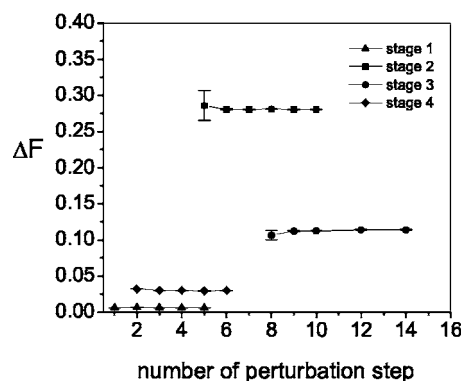


FIG. 2. Dependence of the free-energy difference in each stage on the number of thermodynamic perturbation steps used for the (100) crystal orientation.

reliable result due to its very small free-energy difference. For stage 2 of cleaving liquid and stage 4 of removing cleaving wall, seven and three thermodynamic perturbation steps are enough, respectively. Even for the most complicated stage 3 of forming interface, reliable results can be obtained only by 12 thermodynamic perturbation steps. This is in contrast to thermodynamic integration method where in order to ensure the reversibility of the integration path very small integration increment must be used and many integration steps are needed in each stage.

Finally, we have examined the convergence of the free-energy difference as a function of the sampling size. Figure 3 shows the dependence of the free-energy difference in stage 2 of cleaving liquid on the sampling size for the (100) crystal orientation. From Fig. 3, it can be seen clearly that the result becomes converged and stable very fast. In current work, all the calculations are based on the sampling number of 50 000 nonequilibrium work measurements. For each thermodynamic perturbation step, 20 000 MC steps for stages 1, 2, and 4 and 40 000 MC steps for stage 3 are run for system equilibration, respectively, and 50 000 MC steps are run for data collection. Nonequilibrium works are sampled at every configuration during the run of data collection.

By summing the free-energy differences in the four stages, we obtained the interfacial free energies of different crystal orientations for the Lennard-Jones system. These results can be compared with the results of Davidchack and

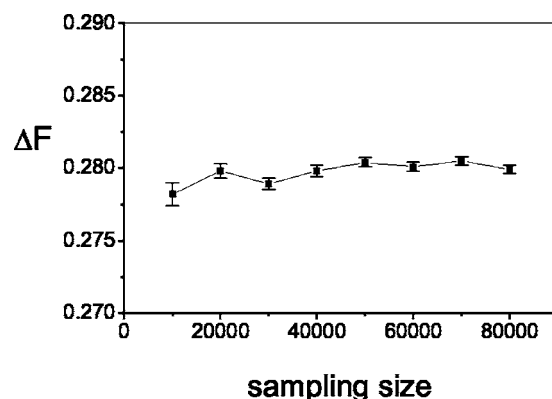


FIG. 3. Dependence of the free-energy difference in stage 2 of cleaving liquid on the sampling size for the (100) crystal orientation.



TABLE II. Comparison with the results of Davidchack and Laird for the interfacial free energies of different crystal orientations. All interfacial free energies are in units of  $\epsilon/\sigma^2$ .

	Current work	Davidchack and Laird
$\gamma_{100}$	$0.371 \pm 0.003$	$0.371 \pm 0.003$
$\gamma_{110}$	$0.361 \pm 0.003$	$0.360 \pm 0.003$
$\gamma_{111}$	$0.354 \pm 0.003$	$0.347 \pm 0.003$

Laird<sup>27</sup> by thermodynamic integration method, which is shown in Table II. As can be seen in Table II, the results of the current work are in very good agreement with the results from Davidchack and Laird using thermodynamic integration method,<sup>27</sup> although there is a small difference in the interfacial free-energy of the (111) crystal orientation. All calculations show that the interfacial free energies are slightly anisotropic and the order of the interfacial free energies of different crystal orientations is  $\gamma_{100} > \gamma_{110} > \gamma_{111}$ .

In addition, it should be noted that there are systematic errors in the cleaving potential technique. The main source of systematic errors is the fluctuations of the interface position in the whole cleaving process, especially in stage 4 where the system contains two interfaces. When the cleaving wall is far from the cleaving plane, the positions of the interfaces cannot be confined at the cleaving plane exactly. In stage 4 of removing the cleaving wall from the system, the interface positions can be disturbed by the process of melting of crystal layers at one interface and simultaneous ordering of liquid at the other interface.

In order to estimate the systematic errors, we performed several independent computations for stage 4 with different perturbation step sizes and took the largest variance as our systematic error. We think that  $0.002\epsilon/\sigma^2$  is a reasonable estimate of systematic error. Compared with the value of statistical error of  $0.001\epsilon/\sigma^2$  which is determined from Bennett's method, the systematic error is larger in the current case. The combinations of statistical and systematic errors are given in Table II as our total error estimate.

## IV. CONCLUSION

In summary, we developed a multistep thermodynamic perturbation method to compute the interfacial free energies by nonequilibrium work measurements with cleaving potential procedure. In order to validate this method, we calculated the interfacial free energies of different crystal orientations for the well-studied Lennard-Jones system near the triple point:  $\gamma_{100} = 0.371 \pm 0.003\epsilon/\sigma^2$ ,  $\gamma_{110} = 0.361 \pm 0.003\epsilon/\sigma^2$ , and  $\gamma_{111} = 0.354 \pm 0.003\epsilon/\sigma^2$ . We find that the anisotropy of the interfacial free-energy is very weak and the anisotropic order is  $\gamma_{100} > \gamma_{110} > \gamma_{111}$ . Our results are in good agreement with the results of Davidchack and Laird<sup>27</sup> using thermodynamic integration method.

Compared with thermodynamic integration method, the multistep thermodynamic perturbation method in this work has two significant merits. First, it is more efficient. For each stage of the cleaving process, only a few thermodynamic perturbation steps are needed. For example, for stage 1 of

cleaving solid, one perturbation step is enough, which could save simulation time and make extensive simulations possible for larger system sizes. Second, it is more reliable. As the free-energy difference is obtained by nonequilibrium work measurements, thus, there is no requirement on the reversibility of the path. Furthermore, the combination of the information from both the forward and reverse paths minimizes the statistical error and there is no hysteresis in the calculations.

This method can be extended to compute other free-energy differences, especially for those situations where it is difficult to use thermodynamic integration method by designing a reversible path. Another possibility to enhance the efficiency of the method is to use multihistogram reweighting method instead of the Bennett method if there are more than one intermediate state.<sup>29</sup>

## ACKNOWLEDGMENT

The authors are grateful for the financial support by a NSF Grant No. CHE0303758.

- <sup>1</sup>A. Pimpinelli and J. Villain, *Physics of Crystal Growth* (Cambridge University Press, Cambridge, 1998).
- <sup>2</sup>J. J. Hoyt, M. Asta, and A. Karma, *Mater. Sci. Eng.*, **R**, **41**, 121 (2003).
- <sup>3</sup>D. Turnbull, *J. Appl. Phys.* **21**, 1022 (1950).
- <sup>4</sup>C. Smits, J. S. van Duijneveldt, J. K. G. Dhont, H. N. W. Lekkerkerker, and W. J. Briels, *Phase Transitions* **21**, 157 (1990).
- <sup>5</sup>S. M. Underwood, J. R. Taylor, and W. van Meegen, *Langmuir* **10**, 3550 (1994).
- <sup>6</sup>D. W. Marr and A. P. Gast, *Langmuir* **10**, 1348 (1994).
- <sup>7</sup>M. E. Glicksman and C. Vold, *Acta Metall.* **17**, 1 (1969).
- <sup>8</sup>R. E. Napolitano, S. Liu, and R. Trivedi, *Interface Sci.* **10**, 217 (2002).
- <sup>9</sup>W. A. Curtin, *Phys. Rev. Lett.* **59**, 1228 (1987).
- <sup>10</sup>W. A. Curtin, *Phys. Rev. B* **39**, 6775 (1989).
- <sup>11</sup>D. W. Marr and A. P. Gast, *Phys. Rev. E* **47**, 1212 (1993).
- <sup>12</sup>R. Ohnesorge, H. Lowen, and H. Wagner, *Phys. Rev. E* **50**, 4801 (1994).
- <sup>13</sup>D. W. Marr, *J. Chem. Phys.* **102**, 8283 (1995).
- <sup>14</sup>V. B. Warshavsky and X. Song, *Phys. Rev. E* (submitted).
- <sup>15</sup>M. D. Lacasse, G. S. Grest, and A. J. Levine, *Phys. Rev. Lett.* **80**, 309 (1998).
- <sup>16</sup>S. W. Sides, G. S. Grest, and M. D. Lacasse, *Phys. Rev. E* **60**, 6708 (1999).
- <sup>17</sup>J. J. Hoyt, M. Asta, and A. Karma, *Phys. Rev. Lett.* **86**, 5530 (2001).
- <sup>18</sup>E. Chacón and P. Tarazona, *Phys. Rev. Lett.* **91**, 166103 (2003).
- <sup>19</sup>J. R. Morris, Z. Y. Lu, Y. Y. Ye, and K. M. Ho, *Interface Sci.* **10**, 143 (2002).
- <sup>20</sup>J. J. Hoyt and M. Asta, *Phys. Rev. B* **65**, 214106 (2002).
- <sup>21</sup>M. Asta, J. J. Hoyt, and A. Karma, *Phys. Rev. B* **66**, 100101(R) (2002).
- <sup>22</sup>J. R. Morris, *Phys. Rev. B* **66**, 144104 (2002).
- <sup>23</sup>J. R. Morris and X. Song, *J. Chem. Phys.* **119**, 3920 (2003).
- <sup>24</sup>Y. Mu and X. Song, *J. Phys. Chem. B* **109**, 6500 (2005).
- <sup>25</sup>J. Q. Broughton and G. H. Gilmer, *J. Chem. Phys.* **84**, 5759 (1986).
- <sup>26</sup>R. L. Davidchack and B. B. Laird, *Phys. Rev. Lett.* **85**, 4751 (2000), and references therein.
- <sup>27</sup>R. L. Davidchack and B. B. Laird, *J. Chem. Phys.* **118**, 7651 (2003).
- <sup>28</sup>C. H. Bennett, *J. Comput. Phys.* **22**, 245 (1976).
- <sup>29</sup>D. Frenkel and B. Smit, *Understanding Molecular Simulation: From Algorithms to Applications* (Academic, San Diego, 1996).
- <sup>30</sup>C. Jarzynski, *Phys. Rev. Lett.* **78**, 2690 (1997).
- <sup>31</sup>G. Hummer, *J. Chem. Phys.* **114**, 7330 (2001).
- <sup>32</sup>N. Lu, J. K. Singh, and D. A. Kofke, *J. Chem. Phys.* **118**, 2977 (2003).
- <sup>33</sup>D. Wu and D. A. Kofke, *J. Chem. Phys.* **121**, 8742 (2004).
- <sup>34</sup>D. Wu and D. A. Kofke, *J. Chem. Phys.* **122**, 204104 (2005).
- <sup>35</sup>H. Oberhofer, C. Dellago, and P. L. Geissler, *J. Phys. Chem. B* **109**, 6902 (2005).
- <sup>36</sup>M. R. Shirts and V. S. Pande, *J. Chem. Phys.* **122**, 144107 (2005).